FISEVIER

Contents lists available at ScienceDirect

Comparative Biochemistry and Physiology, Part C

journal homepage: www.elsevier.com/locate/cbpc



Molecular characterization of novel mitochondrial peroxiredoxins from the Antarctic emerald rockcod and their gene expression in response to environmental warming



A.M. Tolomeo^a, A. Carraro^a, R. Bakiu^b, S. Toppo^c, F. Garofalo^d, D. Pellegrino^d, M. Gerdol^e, D. Ferro^f, S.P. Place^g, G. Santovito^{h,*}

- a Department of Women's and Children's Health, University of Padova, Padova, Italy
- ^b Department of Aquaculture and Fisheries, Agricultural University of Tirana, Tirana, Albania
- ^c Department of Molecular Medicine, University of Padova, Italy
- ^d Departmentof of Biology, Ecology and Earth Sciences (B.E.S.T.), University of Calabria, Arcavacata di Rende, Italy
- ^e Department of Life Sciences, University of Trieste, Trieste, Italy
- f Department of Pharmacology, University of Arizona, Tucson, AZ, USA
- ⁸ Department of Biology, Sonoma State University, Rohnert Park, CA, USA
- h Department of Biology, University of Padova, Padova, Italy

ARTICLE INFO

Keywords: Antarctica Fish Gene expression Global warming Molecular evolution Peroxiredoxins

ABSTRACT

In the present study we describe the molecular characterization of the two paralogous mitochondrial peroxiredoxins from $Trematomus\ bernacchii$, a teleost that plays a pivotal role in the Antarctic food chain. The two putative amino acid sequences were compared with orthologs from other fish, highlighting a high percentage of identity and similarity with the respective variant, in particular for the residues that are essential for the characteristic peroxidase activity of these enzymes. The temporal expression of Prdx3 and Prdx5 mRNAs in response to short-term thermal stress showed a general upregulation of Prdx3, suggesting that this isoform is the most affected by temperature increase. These data, together with the peculiar differences between the molecular structures of the two mitochondrial Prdxs in T. Preparechii as well as in the tropical species Preparechii suggest an adaptation that allowed these poikilothermic aquatic vertebrates to colonize very different environments, characterized by different temperature ranges.

1. Introduction

Fish species occupy a large variety of environments, characterized by very different temperatures. Those inhabiting the Antarctic sea are exposed to year-round low temperatures (Legg et al., 2009): on annual basis, the temperature slightly changes around the average value of $-1.18\,\pm\,0.68\,^{\circ}\text{C}$ (Clark and Peck, 2009). In this peculiar condition, the dissolved oxygen concentration greatly increases in seawaters as well as in tissues and cells (Hardy and Gunther, 1935). Therefore, the formation rate of reactive oxygen species (ROS, i.e. $\cdot\text{O}_2^-$, H_2O_2 and \cdot OH) increases, also increasing the risk of oxidative stress for these animals (Acworth et al., 1997). Reactive oxygen species are physiologically produced in a series of biochemical reactions within cellular compartments (mostly mitochondria and endoplasmic reticulum), but their increased levels may lead to irreversible cell damage and eventually to cell death.

The antioxidant cellular system of all eukaryotic organisms, from yeast to animals, use evolutionarily conserved enzymes and non-enzymatic compounds to limit the presence of ROS, preventing the damages to macromolecules caused by these oxygen derivatives (Boldrin et al., 2008; Ferro et al., 2013, 2017; Formigari et al., 2010; Franchi et al., 2012; Irato et al., 2007; Ricci et al., 2017; Santovito et al., 2015, 2005, 2002). In particular, antioxidant enzymes such as superoxide dismutase (SOD), catalase (CAT), glutathione peroxidase (GPx), methionine sulfoxide reductase (Msr) and peroxiredoxin (Prdx), have a pivotal role in this homeostatic and detoxification system (Ferro et al., 2018).

Peroxiredoxins (Prdxs, EC 1.11.1.15) are a family of peroxidases that reduce H_2O_2 , organic peroxides and peroxynitrite by using cysteine residues that are in the active site as suppliers of reducing equivalents (Konig et al., 2013; Randall et al., 2013; Al-Asadi et al., 2019). In vertebrates, Prdxs are classified into 6 different isoforms, grouped in three subtypes (typical 2-Cys, atypical 2-Cys and 1-Cys) that differ for

^{*} Corresponding author at: via U. Bassi 58/B, 35131 Padova, Italy. E-mail address: gianfranco.santovito@unipd.it (G. Santovito).

their structural and mechanistic features (Wood et al., 2003b).

The typical 2-Cys Prdxs (isoforms from 1 to 4) are obligate homodimers and are identified by the conservation of their two redox-active cysteines, the peroxidatic cysteine and the resolving cysteine (Ren et al., 2014), which form an intermolecular disulfide bond during the enzyme reaction (Hall et al., 2009). The second class of Prdxs are the atypical 2-Cys Prdxs (Prdx5), which have the same mechanism as typical 2-Cys Prdxs but are functionally monomeric, and are characterized by the formation of an intramolecular disulfide bond (Knoops et al., 2011; Wood et al., 2003a). The third subfamily, represented by Prdx6, includes the 1-Cys Prdxs. It is a bifunctional protein, catalyzing similar chemical reactions as glutathione peroxidase and phospholipase A2 (PLA2) (Liu et al., 2015; Rahaman et al., 2012).

Although Prdxs have received considerable attention in recent years, due to their role as important cellular antioxidant proteins that help control intracellular peroxide levels, only two Prdx6 genes have been studied until now in *Trematomus bernacchii* (Tolomeo et al., 2016), a teleost widely distributed in many areas of Antarctica.

In the present work, aimed at characterizing the mitochondrial Prdxs of *T. bernacchii*, we report on the molecular characterization of two novel subtypes: Prdx3 occurring exclusively within mitochondria (Chae et al., 1999) and Prdx5 that is also distributed in several other cellular compartments, such as peroxisomes (Kropotov et al., 1999; Seo et al., 2000). The interest in mitochondrial isoforms of Antarctic fish is related to the unique metabolic adaptation observed in these organisms, which include an increased mitochondrial density (Johnston et al., 1998; Pörtner et al., 2005).

In order to evaluate the relationships between the molecular diversification of Antarctic Prdxs and the evolutionary history of cold-adapted teleosts, we compared the sequence of the newly characterized Prdxs from *T. bernacchii* with those from other vertebrate species. The evolution of Prdxs is particularly interesting, since they are considered ancient proteins, which are thought to have evolved by gene duplication events during the past 2.5 billion years, in parallel with other components of ROS detoxifying systems and metabolic pathways. Furthermore, we employed molecular modeling techniques to predict the structure of the two cold-adapted Prdx3 and Prdx5. In particular, using various in silico approaches, we investigated Antarctic fish mitochondrial Prdxs (i.e., compared with other, non-cold-adapted, mitochondrial Prdxs), with the aim to identify molecular characteristics consistent with cold adaptation.

Finally, to obtain further information on the physiological role of mitochondrial Prdxs in *T. bernacchii*, we characterized basal mRNA expressions of both Prdx3 and Prdx5 isoforms in various organs and tissues. We also analyzed changes in gene expression for both Prdx genes after exposure to short-term thermal stress to gain a better understanding of their potential role in the response of *T. bernacchii* to the global climate warming related sea temperature increase.

2. Material and methods

2.1. Ethical procedures

The sample collection and animal research conducted in this study comply with Italy's Ministry of Education, University and Research regulations concerning activities and environmental protection in Antarctica and with the Protocol on Environmental Protection to the Antarctic Treaty, Annex II, Art. 3. All experiments have been performed in accordance with the U.K. Animals (Scientific Procedures) Act, 1986 and associated guidelines, EU Directive 2010/63/EU for animal experiments.

2.2. Experimental animals

Adult samples of *T. bernacchii* were collected in the proximity of Mario Zucchelli Station in Terra Nova Bay, Antarctica (74°42′S,

167°7′E) and kept in aquaria supplied with aerated seawater at approximately 0 °C. Five specimens were immediately euthanized (tricainemethanesulfonate, MS-222; $0.2\,\mathrm{g\,I^{-1}}$) and samples of liver, heart, spleen and skeletal muscle tissues were quickly excised, placed into cryotubes, snap-frozen in liquid nitrogen and later stored at $-80\,^{\circ}$ C. To measure changes in mRNA abundance after a short thermal stress, we acclimated 25 specimens to a gradual increase in seawater temperature from 0 °C to 5 °C. The water temperature in the aquariums was increased at a rate of $0.05\,^{\circ}$ C/h until it reached the next degree centigrade. At 1 °C, 2 °C, 3 °C, 4 °C and 5 °C, the water temperature was held constant for four days, after which five specimens were sacrificed, tissue samples quickly removed, frozen in liquid nitrogen, and stored at $-80\,^{\circ}$ C until they were analyzed. Twenty-five untreated specimens were maintained at a control temperature of 0 °C and n=5 fish were sacrificed at the same times as the warm acclimated specimens.

2.3. Primers design, RNA extraction, synthesis, cloning and sequencing of Prdx3 and Prdx5 cDNAs

For primer design, amino acid and nucleotide sequences of Prdx3 and Prdx5 from fish were obtained from NCBI database and aligned by MUSCLE (Edgar, 2004). The considered fish species include *Sparus aurata* (Gilt-head seabream), *Danio rerio* (Zebrafish), *Miichthys miiuy* (Miiuy croaker), *Oreochromis niloticus* (Nile tilapia), *Maylandia zebra* (Zebra Malawi Cichlid), *Oryzias latipes* (Japanese ricefish), *Takifugu rubripes* (Japanese pufferfish) and *Salmo salar* (Atlantic salmon). The primers were designed in the conserved domains and the primer sequences were analyzed with IDT Oligo analyzer (http://eu.idtdna.com/analyzer/Applications/OligoAnalyzer/). Primer sets are shown in Table S1.

Total RNA was purified from various tissues of *T. bernacchii* using TRIzol® reagent (Invitrogen) according to the manufacturer's protocol. Total RNA was further purified with 8 M LiCl in order to remove glucidic contaminants (Ferro et al., 2015) and the quantification was performed using the ND-1000 spectrophotometer (Nanodrop, Wilmington, DE); RNA integrity was assessed by capillary electrophoresis using the Agilent Bioanalyzer 2100, with the RNA 6000 Nano (Agilent Technologies, Palo Alto, CA). The first strand of cDNA was reverse-transcribed at 42 °C for 1 h from 1 μ g of total RNA in a 20 μ L reaction mixture, containing 1 μ L of ImProm-II™ Reverse Transcriptase (Promega) and 0.5 μ g oligodT Anchor primer. PCR reactions were performed with 50 ng of cDNA. The PCR program was the following: 95 °C for 2 min and 35 × (95 °C for 30 s, Tm for 30 s, 72 °C for 1 min); final elongation 72 °C for 10 min T_ms are shown in Table S1.

All the amplicons were gel-purified with the NucleoSpin Extract 2 in 1 (Macherey-Nagel), ligated into the pGEM*-T Easy Vector (Promega) and cloned in XL1-Blue *E. coli* cells (Invitrogen). Positively screened clones were sequenced at the BMR Genomics (University of Padova) on an ABI PRISM 3700 DNA Analyzer (Applied Biosystems).

2.4. Semiquantitative RT-PCR (sqRT-PCR) analysis

In order to evaluate expression of mitochondrial Prdx mRNAs, semiquantitative RT-PCR (sqRT-PCR) analysis was performed. cDNAs for Prdx3 and Prdx5 were amplified with the specific primers reported in Table S1. To control for variation in efficiency of cDNA synthesis and PCR amplification reactions, the housekeeping gene β -actin from *T. bernacchii* (GenBank accession number: ADF45299.1) was used as a control and amplified with species-specific primers (Table S1). PCR amplifications were carried out with the following program: 95 °C for 2 min, then a variable number of cycles of 95 °C for 30 s, 30 s at specific melting temperature (Table S1), 72 °C for 1 min. For all the genes, the number of amplification cycles was optimized (35 for Prdx3 and Prdx5, 40 for β -actin) to ensure that PCR products were quantified during the exponential phase of the amplification.

The amplification products were separated by electrophoresis on

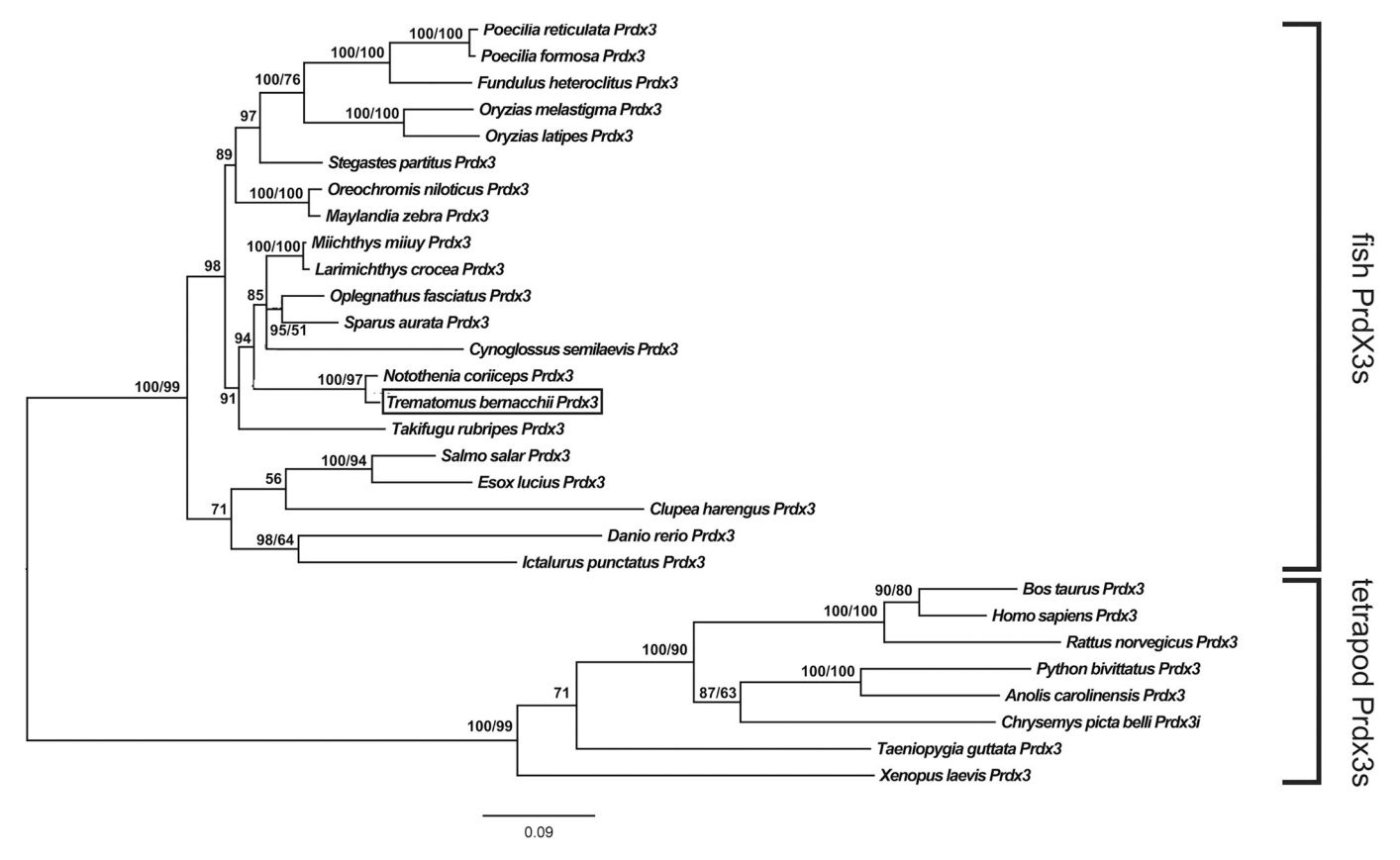


Fig. 1. Phylogenetic relationships among Prdx3s of various organisms, reconstructed on the basis of cDNA coding region sequences and using both methods: BI (arithmetic mean = -9886.08; harmonic mean = -9910.49) and ML (arithmetic mean = -9790.69). Bayesian posterior probability (first number) and bootstrap values higher than 50% are indicated on each node, respectively. The scale for branch length (0.09 substitution/site) is shown below the tree. *T. bernacchii* Prdx3 is boxed.

1.5% agarose GelRed-stained gel (Biotium) and the relative intensities were quantified with the software Quantity-one through a quantitative ladder (Gene RulerTM, Fermentas). Transcript levels are reported as the intensity (in arbitrary units, a.u.) of the gene of interest relative to the expression level of β -actin in the same sample.

2.5. Statistical analysis

All data were expressed as the average of five analyzed specimens \pm standard deviation (SD). Statistical analyses were performed with the PRIMER statistical program. One-way ANOVA was followed by the Student–Newman–Keuls test to assess significant differences (p < 0.05).

2.6. Phylogenetic analyses

Phylogenetic studies were based on both amino acid and nucleotide sequences of Prdx3 and Prdx5 from *T. bernacchii* and other species available in GenBank database (Tables S2 and S3).

The T-Coffee multiple sequence alignment package has been used to obtain multiple sequence alignment of Prdx3 and Prdx5 sequences (Notredame et al., 2000). Even though this method is based on the popular progressive approach to multiple alignment, we decided to use it because it is characterized by a dramatic improvement in accuracy with a modest sacrifice in speed, as compared to the most commonly used alternatives (Notredame et al., 2000).

The jModelTest 2.0 software (Darriba et al., 2012) was used to carry out statistical selection of best-fit models of nucleotide substitution. Analyses were performed using 88 candidate models and three types of information criterion (Akaike Information Criterion - AIC, Corrected

Akaike Information Criterion - cAIC and Bayesian Information Criterion - BIC). To select the best-fit model of analyzed protein evolution ProtTest 3 was used (Darriba et al., 2011). One hundred and twenty-two candidate models and the three previously mentioned criteria were used in these statistical analyses.

Phylogenetic trees were built using the Bayesian inference (BI) method implemented in Mr. Bayes 3.2 (Ronquist et al., 2012). Four independent runs, each one with four simultaneous Markov Chain Monte Carlo (MCMC) chains, were performed for 500,000 generations sampled every 1000 generations. Furthermore, we also used the maximum likelihood (ML) method implemented in PhyML 3.0 (Guindon et al., 2010). Bootstrap analyses were performed on 100,000 trees using both kinds of tree topology improvement: nearest neighbor interchange (NNI) and subtree pruning and regrafting (SPR). FigTree v1.3 software was used to display the annotated phylogenetic trees.

Finally, we employed the mechanistic empirical model (MEC) (Doron-Faigenboim and Pupko, 2007) that accounts for the different amino acid replacement probabilities based on the WAG empirical substitution matrix, while estimating the codon rate matrix, thus allowing for positions undergoing radical amino acid exchanges to acquire higher dN rates than those with less radical exchanges. The codonwise × estimates were mapped onto bovine (pdb: 4MH2) and human (pdb: 3MNG) protein tertiary structures using the Selecton-3D web server (http://selecton.tau.ac.il).

2.7. Molecular modeling

Structural models were obtained for isoforms of Prdx3 from *Notothenia coriiceps, Stegastes partitus* and *T. bernacchii*. The template used for molecular modeling were the crystal structure of bovine

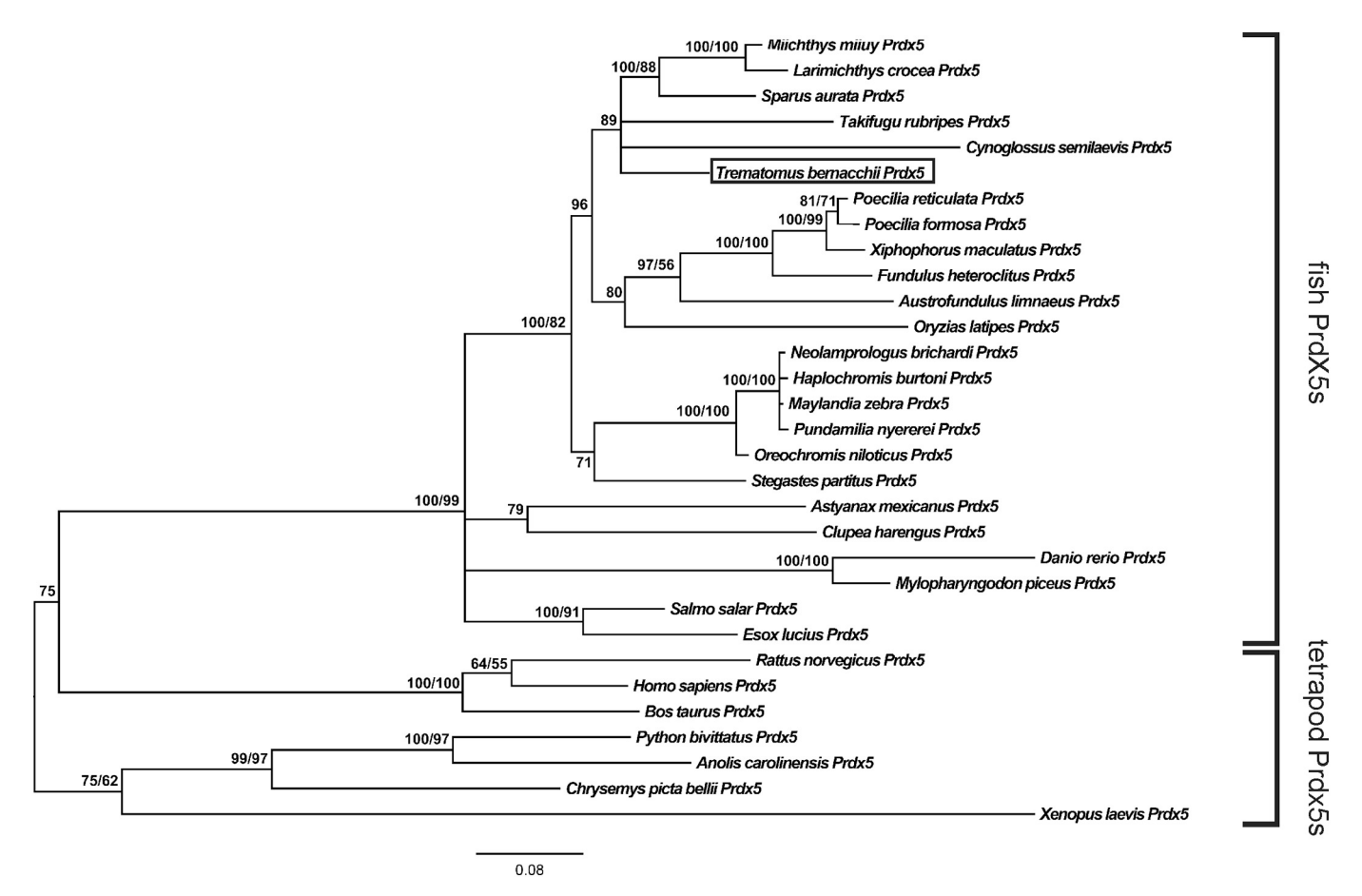


Fig. 2. Phylogenetic relationships among Prdx5s of various organisms, reconstructed on the basis of cDNA coding region sequences and using both methods: BI (arithmetic mean = -8929.78; harmonic mean = -8960.92) and ML (arithmetic mean = -8848.95). Bayesian posterior probability (first number) and bootstrap values higher than 50% are indicated on each node, respectively. The scale for branch length (0.08 substitution/site) is shown below the tree. *T. bernacchii* Prdx5 is boxed.

mitochondrial peroxiredoxin III (pdb: 4MH2) sharing 84.54%, 86.08% and 84.02% identity with *N. coriiceps, S. partitus* and *T. bernacchii* protein sequences, respectively.

Structural models were also built for isoforms of Prdx5 from *S. partitus* and *T. bernacchii*. In this case the template used for molecular modeling was the crystal structure of the wild type human peroxiredoxin V (pdb: 3MNG) sharing 71.25% and 71.88% identity with *S. partitus* and *T. bernacchii* protein sequences, respectively.

Final models were built with SWISS-MODEL (Biasini et al., 2014) and further energy minimized with GROMACS 5.04 (http://www.gromacs.org/) software package using Amber ff99SB-ILDN (Lindorff-Larsen et al., 2010) force field. The systems were subjected to a steepest descent energy minimization until reaching a tolerance force of no greater than $1000\,\mathrm{kJ}\,\mathrm{mol}^{-1}\,\mathrm{nm}^{-1}$. Electrostatic surface potential was calculated for the energy minimized models using the programs PDB2PQR (Dolinsky et al., 2007) and APBS (Baker et al., 2001), with the nonlinear Poisson-Boltzmann equation and contoured at \pm 3 kT/e.

3. Results

3.1. Organization of T. bernacchii Prdx3 and Prdx5 genes

Cloning and sequencing from *T. bernacchii* liver yielded a partial cDNA sequence of Prdx3. This sequence was compared with the recently published head kidney *T. bernacchii* transcriptome database (Gerdol et al., 2015), that allowed us to obtain the full-length cDNA sequence (GenBank accession number KU207097). In silico analyses carried out on the muscle *T. bernacchii* transcriptome database, recently

assembled with transcriptomes from liver, gills and brain (Huth and Place, 2013), allowed us to identify the presence of a *prdx5* transcript (GenBank accession number KU308347).

The *prdx3* transcript is 972 nt long. The 5′- and 3′-UTR regions consist of 108 nt and 117 nt, respectively. The open reading frame (ORF) includes 747 nt and encodes a putative protein of 248 aa, with a deduced molecular weight of 26.9 kDa (Fig. S1). The 3′-UTR region includes a putative polyadenylation signal (AATAAA) at 853–858 nt.

The Prdx5 transcript is 1074 nt long. The 5'- and 3'-UTR regions consist of 223 nt and 278 nt, respectively. The ORF includes 573 nt and encodes a putative protein of 190 aa, with a deduced molecular weight of 20.2 kDa (Fig. S2). The 3'-UTR region includes a putative polyadenylation signal (AATAAA) at 820–825 nt and two ATTTA sequences, at nt 709–713 and 934–938, which signal rapid degradation in certain mammalian mRNAs (Shaw and Kamen, 1986).

The amino acid sequences of Prdx3 of *T. bernacchii* show the highest identity (96.8%) and similarity (99.2%) with the Prdx3 of *N. coriiceps* (order Perciformes; Table S4). On the other hand, the Prdx5 of *T. bernacchii* shows the highest sequence identity (87.4%) and similarity (98.9%) with the Prdx5 of *Sparus aurata* (order Perciformes; Table S5).

3.2. Phylogenetic analyses and molecular modeling

The jModelTest 2.0 software determined the GTR + I + G model as the best-fit model of molecular evolution for Prdx3 and Prdx5 at the cDNA level, with gamma shape values (four rate categories) of 0.985 and 1.042, respectively, using all statistical criteria ($-\ln L = 19,127.40$ for Prdx3 and $-\ln L = 8894.77$ for Prdx5). The phylogenetic

```
Prdx3: Trematomus bernachii
                                    MAASIGRLLRTSVKVAAG----GLKVTASCQRGASGAR---RILSTPSLQRAGFSTSSSR
                                    MAASVGTLMRTCARVAAG----SLKLTVASQHGVSGAA---RVLTAPALQRACFSTSSCR
Prdx3: Cynoglossus semilaevis
                                    MAASIGRLLRTSAKVAAG----GLKVTASCQHGASGAR---RILSAPSLQRAGFATSSSR
Prdx3: Notothenia coriiceps
                                    MAATIGRLLRTSALVAAG----GLKVTPACQRVASATA---RALTGPALQRACFSTNTSR
Prdx3: Takifugu rubripes
                                    MAATIGRLLRTSARVAAG----GLKVPAACOPGASGAA---RILTGPALORACFSTSTSR
Prdx3: Oplegnathus fasciatus
Prdx3: Miichthys miiuy
                                    MAATIGRLLRTSASVAAG----GLKVTAASRHGASGAV---RALTAPALQRACFSTSTSR
                                    MAATIGRLLRTSASVAAG---GLNVTAASRHGASGAV---RALTAPALQRACFSTSTSR
Prdx3: Larimichthys crocea
Prdx3: Stegastes partitus
                                    MAATVGNLLRTSARVAAG----GLKVAAAROHAACGAA---RVLAAPALORTCFSTTTSR
                                    MAATIGKLLRTSARVAAG----GLKVAAACQHGACGAA---RVLTAPALQRSRFSTSASR
Prdx3: Oreochromis niloticus
                                    MAATIGKLLRTSARVAAG----GLKVAAACQHGACGAA---RVLTAPALQRSCFSTSASR
Prdx3: Maylandia zebra
Prdx3: Fundulus heteroclitus
                                    MASTVHRLLRTSVRVAAG----GLKAAAAYOHGAGGSA---RVLSAAACORSFFSTGTSR
Prdx3: Poecilia reticulata
                                    MAATVGRLLRTSVQVAAG----GLKVAAACQHGVGGAA---RVLSAPVLQKSFFSTGSSR
                                                           .*: :: . .:
Prdx3: Homo sapiens
                                    MAAAVGRLLRASVARHVSAIPWGISATAALRPAACGRTSLTNLLCSGSSOAKLFSTSSSC
Prdx3: Trematomus bernachii
                                    WAPAVTQAAPDFKGTAVSNGEFKEMSLADFKGKYLVLFFYPLDFTFVCPTEIISFSDKAN
Prdx3: Cynoglossus semilaevis
                                    WAPAVTQPAPAFKATAVHNGEFKEMSLGDFKGKYLVLFFYPLDFTFVCPTEIISFSDKVN
Prdx3: Notothenia coriiceps
                                    WAPAVTQAAPDFKGTAVSNGEFKEMSLADFKGKYLVLFFYPLDFTFVCPTEIISFSDKAN
Prdx3: Takifugu rubripes
                                    —
WAPAVTQPAPAFKGTAVHNGEFKEMSLADFKGKYLVLFFYPLDFTFVCPTEIIAFSDKAN
                                    WAPAVTHPAPAFKATAVHNGEFKEMSLADFKGKYLVLFFYPLDFTFVCPTEIISFSDKAS
Prdx3: Oplegnathus fasciatus
Prdx3: Miichthys miiuy
                                    WTPAVTQPAPAFKATAVHNGEFKEMSLADFKGKYLVLFFYPLDFTFVCPTEI SFSDKAN
Prdx3: Larimichthys crocea
                                    WTPAVTQPAPAFKATAVHNGEFKEMSLADFKGKYLVLFFYPLDFTFVCPTEIISFSDKAN
                                    WAPAVTQPAPAFKATAVHNGEFKEMSLADFKGKYLVLFFYPLDFTFVCPTEIIAFSDKAN
Prdx3: Stegastes partitus
                                    WAPAVTQPAPAFKGTAVHNGEFKDMSLADFKGKYLVLFFYPLDFTFVCPTEIIAFSDKAN
Prdx3: Oreochromis niloticus
Prdx3: Maylandia zebra
                                    —
WAPAVTQPAPAFKGTAVHNGEFKDMSLADFKGKYLVLFFYPLDFTFVCPTEIIAFSDKAN
                                    WAPAVTQPAPDFKATAVHNGEFKDLRLADFKGKYLVLFFYPLDFTFVCPTEIISFSDMAK
Prdx3: Fundulus heteroclitus
                                    WAAAVTQPAPGFKATAVHNGEFKDLSLADFKGKYLVLFFYPLDFTFVCPTEIISFSDKAK
Prdx3: Poecilia reticulata
                                    *: ***: ** **.*** *****:: *.*******
                                    HAPAVTQHAPYFKGTAVVNGEFKDLSLDDFKGKYLVLFFYPLDFTFVCPTEIVAFSDKAN
Prdx3: Homo sapiens
Prdx3: Trematomus bernachii
                                    EFHDVNCEVVGVSVDSHFTHLAWINTPRKTGGLCHIHIPLLSDLNKQISKDYGVLLEGPG
                                    EFHDINCEVVGVSVDSHFTHLAWINTPRKTGGLENIKIPLLSDLTKQISRDYGVLLENPG
EFHDVNCEVVGVSVDSHFTHLAWINTPRKTGGLEHIHIPLLSDLNKQISKDYGVLLEGAG
Prdx3: Cynoglossus semilaevis
Prdx3: Notothenia coriiceps
Prdx3: Takifugu rubripes
                                    EFHDVNCEVVGVSVDSHFTHLAWINTPRKTGGLGHIHIPLLSDLTKQISRDYGVLLEGPG
                                    EFHDVNCEVVGVSVDSHFTHLAWINTPRKTGGLENIHIPLLSDLTKQISRDYGVLLEGPG
EFHDVNCEVVGVSVDSHFTHLAWINTPRKTGGLEHIHIPLLSDLNKQISRDYGVLLEGPG
Prdx3: Oplegnathus fasciatus
Prdx3: Miichthys miiuy
Prdx3: Larimichthys crocea
                                    EFHDVNCEVVGVSVDSHFTHLAWINTPRKTGGLGHIHIPLLSDLNKQISRDYGVLLEGPG
Prdx3: Stegastes partitus
                                    EFHDVNCEVVGVSVDSHFTHLAWINTPRKTGGLGHIHIPLLSDLNKQISRDYGVLLEGPG
                                    EFHDVNCEVVGVSVDSHFTHLAWINTPRKAGGLGNIHIPLLSDLNKQISRDYGVLLDGPG
Prdx3: Oreochromis niloticus
Prdx3: Maylandia zebra
                                    EFHDVNCEVVGVSVDSHFTHLAWINTPRKAGGLGNIHIPLLSDLNKQISRDYGVLLDGPG
Prdx3: Fundulus heteroclitus
                                    EFHDVNCEVVGVSVDSHFTHLAWINTPRKAGGLGNIHIPLLSDLSKQISRDYGVLLESPG
Prdx3: Poecilia reticulata
                                    EFHDVNCEVVGVSVDSHFTHLAWINTPRKAGGLGNIHIPLLSDLNKQISRDYGVLLDGPG
                                    Prdx3: Homo sapiens
                                    EFHDVNCEVVAVSVDSHFSHLAWINTPRKNGGLCHMNIALLSDLTKQISRDYGVLLEGSG
                                    IALRGLFLIDPNGVVRHMSVNDLPVGRCVEETLRLVKAFQFVETHGEVCPASWTPDSPTI
Prdx3: Trematomus bernachii
Prdx3: Cynoglossus semilaevis
                                    IALRGLFIIDPNGVVRHTSVNDLPVGRSVEETLRLVKAFQFVETHGEVCPASWTPKSPTI
                                    IALRGLFLIDPNGVVRHMSVNDLPVGRCVEETLRLVKAFQFVETHGEVCPASWTPESPTI
Prdx3: Notothenia coriiceps
                                    IALRGLFVIDPSGVVKHMSINDLPVGRSVEETLRLVKAFQFVETHGEVCPASWTPESPTI IALRGLFIIDPNGVVKHMSVNDLPVGRSVEETLRLVKAFQFVETHGEVCPASWTPKSPTI
Prdx3: Takifugu rubripes
Prdx3: Oplegnathus fasciatus
                                    IALRGLFIIDPNGVVKHMSVNDLPVGRCVEETLRLVKAFQFVETHGEVCPASWTPNSPTI
Prdx3: Miichthys miiuy
                                    IALRGLFIIDPNGVVKHMSVNDLPVGRCVEETLRLVKAFQFVETHGEVCPASWTPNSPTI IALRGLFIIDPNGIVKHLSVNDLPVGRCVEETLRLVKAFQFVETHGEVCPASWTPKSPTI
Prdx3: Larimichthys crocea
Prdx3: Stegastes partitus
                                    IALRGLFIIDPNGVVKHMSVNDLPVGRCVEETLRLVKAFQFVETHGEVCPASWTPHSPTI
Prdx3: Oreochromis niloticus
                                    IALRGLFIIDPNGVVKHMSVNDLPVGRCVEETLRLVKAFQFVETHGEVCPASWTPHSPTI
IALRGLFIIDPNGVVKHMSINDLPVGRSVEETLRLVKAFQFVETHGEVCPASWTPKSPTI
Prdx3: Maylandia zebra
Prdx3: Fundulus heteroclitus
                                    IALRGLFIIDPNGVVKHMSVNDLPVGRSVEETLRLVKAFQFVETHGEVCPASWTPKSPTI
Prdx3: Poecilia reticulata
                                    ************
                                    LALRGLFIIDPNGVIKHLSVNDLPVGRSVEETLRLVKAFQYVETHGEVCPANWTPDSPTI
Prdx3: Homo sapiens
                                    KPTPEGSKEYFEOVN-
Prdx3: Trematomus bernachii
Prdx3: Cynoglossus semilaevis
                                    KPTPEGSKEYFEKVN-
Prdx3: Notothenia coriiceps
                                    KPTPEGSKEYFEKVN-
Prdx3: Takifugu rubripes
                                    KPTPEGSKEYFGKVN-
Prdx3: Oplegnathus fasciatus
                                    KPTPEGSKEYFEKVN-
Prdx3: Miichthys miiuy
                                    KPTPDGSKEYFEKVN-
Prdx3: Larimichthys crocea
                                    KPTPDGSKEYFEKVN-
Prdx3: Stegastes partitus
                                    KPTPEGSKEYFEKVN-
Prdx3: Oreochromis niloticus
                                    KPTPEGSKEYFEKVN-
Prdx3: Maylandia zebra
                                    KPTPEGSKEYFEKVN-
Prdx3: Fundulus heteroclitus
                                    KPTPEGSKEYEEKVN-
Prdx3: Poecilia reticulata
                                    KPTPEGSKEYFEKVN-
                                    **** *** **
                                    KPSPAASKEYFQKVNQ
Prdx3: Homo sapiens
```

Fig. 3. Multiple alignment of the amino acid sequences of 12 Prdx3s from Teleost species as well as from Homo sapiens. The catalytic center for peroxidase activity is boxed in continuous. The amino acid residues highlighted in dark grey represent the peroxidase triad. The peroxidatic and the resolving cysteines are highlighted in light grey. Two structural motifs which confer sensitivity to inactivation by hydrogen peroxide are boxed in dotted line. In bold is the Threonine responsible for the enzyme phosphorylation. Mitochondrial targeting signal is underlined. The symbols at the bottom of the Teleost sequences correspond to the definitions of the MUSCLE program: (*) fully conserved; (.) highly conserved; (.) conserved substitution.

relationships among Prdx3 and Prdx5 cDNA sequences were determined using the most powerful statistical method of BI. BI and maximum likelihood (ML) methods generate phylogenies with the same topology, depicted in the cladogram of Figs. 1 and 2.

T. bernacchii Prdx3 was placed in the fish Prdx3 cluster, well separated from the Prdx3s from other vertebrates (posterior probability 100%; bootstrap values 99%; Fig. 1). In particular, consistent with the aforementioned high sequence similarity with the N. coriiceps sequence, the two Antarctic Prdx3 sequences were clustered together (posterior probability 100%; bootstrap values 97%). The cluster including the orthologous proteins from Miichthys miiuy, Larimichthys crocea, Oplegnathus fasciatus, Sparus aurata (order Perciformes) and Cynoglossus semilaevis (order Pleuronectiformes) can be identified as the sister group of Antarctic fish Prdx3s.

T. bernacchii Prdx5 was placed in the fish Prdx5 cluster, which is clearly separated from the tetrapod Prdx3 cluster (posterior probability 100%; bootstrap values 99%; Fig. 2). In particular, the T. bernacchii sequence is related to Prdx5 from Miichthys miiuy, Larimichthys crocea, Sparus aurata (order Perciformes), Takifugu rubripes (order Tetraodontiformes) and Cynoglossus semilaevis (order Pleuronectiformes; posterior probability 89%).

The ProtTest3 analysis determined the JTT + G model as the best-fit model of molecular evolution for Prdx3 and Prdx5 at the amino acid level, with gamma shape values (four rate categories) of 0.632 and 0.512, respectively, using all statistical criteria ($-\ln L = 8050.09$ for Prdx3 and $-\ln L = 3991.37$ for Prdx5). BI and ML methods generate phylogenies with the same topology, depicted in the cladogram shown in Figs. S3 and S4.

Again, *T. bernacchii* Prdx3 was placed in a cluster, that includes all known fish Prdx3s. Furthermore, the phylogenetic relationships among the various Prdx3 sequences are quite confirmed, even if with a lower degree of resolution. One difference is the relationships between Antarctic fish Prdx3s and the orthologous sequence from *Sparus aurata* (posterior probability 100%; bootstrap values 65%; Fig. S3).

T. bernacchii Prdx5 was placed within the fish Prdx5 cluster, which is clearly separated from the tetrapod Prdx5s (posterior probability 100%; bootstrap values 100%; Fig. S4). The phylogenetic relationships among the various fish Prdx5 sequences are confirmed, although with a lower degree of resolution.

The MEC analysis indicated a strong prevalence of negative selection in the evolution of fish Prdx3s, even though some amino acid residues have been subject to significant positive selection along evolution (Fig. S5). In fact, this analysis highlighted positive selection for Leu²⁴, Arg²⁷, Val³⁰, Val³², Pro³⁸, Ile⁴² and Lys²³¹ (with reference to zebrafish Prdx3 for residue numbering). Similarly, the MEC analysis indicated a low prevalence of positively selected sites in fish Prdx5s (Fig. S6). In fact, the only identified positively selected residues are Thr⁴, Leu⁷, Ala¹⁴, Ser¹⁶, Ile²⁵, Thr²⁶, Hys³⁵ and Gly⁸⁷ (with reference to black carp Prdx3 for residue numbering).

The multiple sequence alignment among the deduced amino acid sequences of Prdx3 from T. bernacchii, other fish species and Homo sapiens shows a high conservation of the amino acids that are essential for peroxidase activity (Fig. 3). In particular, the most well-conserved sites across all species are the peroxidatic and the resolving cysteines $(Cys^{101}$ and Cys^{222} , respectively), which are present in the functional motifs FYPLDFTFVCPTEI and GEVCPA. The former motif also includes highly conserved residues $(Pro^{94}$ and $Thr^{98})$ which are part of the catalytic triad. The third residue of the catalytic triad (Arg^{147}) , was also invariably conserved, as well as the amino acid responsible for enzyme

phosphorylation (Thr¹³⁹) and two structural motifs (GGLG and YF) which confer to this protein its characteristic sensitivity to inactivation by hydrogen peroxide. The N-terminal region, representing the mitochondrial targeting signal, appears to be poorly conserved.

Fig. 4 displays the multiple sequence alignment among the deduced amino acid sequences of *T. bernacchii* Prdx5 and orthologues from other fish species, with the addition of *Homo sapiens*. As in the case of Prdx3, the peroxidatic and the resolving cysteines (Cys⁷⁵ and Cys¹⁸⁰, respectively), as wells as the residues of the catalytic triad (Pro⁶⁸, Thr⁷² and Arg¹⁵³) are fully conserved. Both the N- and C-terminal portions of the protein, representing the signals for protein sorting to mitochondrion and peroxisome, respectively, display a low degree of conservation.

T. bernacchii Prdx3 is characterized by six specific substitutions, which involve amino acids that are not included in the catalytic group: Pro⁶¹ is substituted by Ala; His⁷¹ is substituted by Ser; Arg¹⁶³ is substituted by Lys; Asp replaces Lys, Glu, Asn or His in position 229; Lys²⁴⁶ is substituted by Gln. The first three substitutions are also present in *N. coriiceps*, which belongs to the same Family (Nototheniidae). *T. bernacchii* Prdx5 shows three specific substitutions, namely: Met replacing Ile or Val in position 95; Val¹²² that is substituted by Ile; Leu¹⁶⁰ that is substituted by Val.

The electrostatic surfaces of Prdx3 models display a strongly negative contour, as shown in Fig. 5, and total net charges of the homodimers range from -9 of T. bernacchii and N. coriceps (panels A and B) to -7 of S. partitus (panel C). Similarly, the Prdx5 models show that monomer is negatively charged (although at less extent), displaying a net charge ranging from -2 in T. bernacchii to -1 in S. partitus, respectively (Fig. 5C–D).

3.3. Analysis of gene expression in natural condition and after increased environmental temperature

Basal mRNA expression levels were determined in heart, liver, spleen and skeletal muscle of non-stressed specimens of T. bernacchii to characterize the tissue specific expression patterns of Prdx3 and Prdx5. Fig. 6 shows that both genes are expressed at high levels in liver and heart. These tissues displayed a Prdx3 mRNA expression approximately 2- and 4-fold higher than skeletal muscle and spleen, respectively (p < 0.05; Fig. 6A). The difference observed between these two organs was statistically significant (p < 0.05). Prdx5 displayed a much more uniform pattern of expression across tissues, with liver and heart showing similar levels of expression, about 1.5-fold higher than spleen and muscle (p < 0.05; Fig. 6B).

Based on these results, we focused our attention on liver and heart tissues for the subsequent analyses of gene expression in specimens exposed to experimental thermal stress. Another main factor which led to the selection of these two tissues was their physiological roles in processes such as detoxification (liver) and oxidative metabolism (hearth), which are related to ROS production. In liver, the transcription of prdx3 showed a significant increase when the temperature reached +2 °C. Subsequent temperature increments did not lead to any further significant increase of mRNA expression. The group subject to thermal stress displayed mRNA levels 1.6-fold higher (p < 0.001) than control specimens for all considered temperatures (Fig. 7A). On the other hand, mRNA levels remained stable throughout the entire experiment in control animals. Although mRNA levels of prdx5 observed in specimens exposed to elevated temperatures were slightly lower than controls, these differences were not statistically significant (Fig. 7B). As in the case of prdx3, prdx5 expression remained stable in the control

D 1 F	manage to a second and the	MICIEDELENGEDIA	0.0	THE THEODIEN DIOLOGO
	Trematomus bernacchii			<u>VKLLHTSPVVKM</u> -PIQVGE
	Cynoglossus semilaevis			<u>VKLLHTSAVARM</u> -PIQVGE
	Takifugu rubripes Fundulus heteroclitus	MFSTAASLLKAPRAL		ARLLRSSPASKM-PIQVGE
	Xiphophorus maculatus			·VRLLHCSPVTKM-PIKVGE
	Poecilia reticulata	MFSITGSLLKTPRVL		XRLLHCSPVIKM-PIKVGE
	Poecilia formosa			VRLLHCSPVTKM-PIKVGE
	Stegastes partitus			VRLLHITPVAKM-PIOIGE
	Oreochromis niloticus			ARLLHITPTTKM-PIQVGE
	Neolamprologus brichardi			ARLLHITPTSKM-PIQVGE
	Haplochromis burtoni	MLPVTSAVLRSSRVL		ARLLHITPTSKM-PIQVDE
	Maylandia zebra			ARLLHITPTSKM-PIQVGE
	Pundamilia nyererei	MLPVTSAVLRSSRVL		ARLLHITPTSKM-PIQVGE
	Sparus aurata	MLSITGSLIKNTRVV		VRLLHTSPIARM-PIQVGE
	Miichthys miiuy	MLFVTATLNKSARVV		LRLLHSSPIAKM-PIQVGE
	Larimichthys crocea	MLSVTATLNKTGRVL		LRLLHSSPTAKM-PIOVGE
iiuxs.	Dallinienenys Clocea	*: : : : *	:	:**: : :* **::
Prdx5:	Homo sapiens	MGLAGVCALRRSAGYILVGGAG	GQSAAAAAARRCSEGE	WASGGVRSFSRAAAAMAPIKVGD
	Trematomus bernacchii			PGCSKTHLPGFVEQAADLKSKGM
	Cynoglossus semilaevis			PGCSKTHLPGFVSQAADLKKKGI
	Takifugu rubripes			PGCSKTHLPGFVQQAEDLKAKGV
	Fundulus heteroclitus	~ ~		PGCSKTHLPGFVQQAEELRSKGI
	Xiphophorus maculatus			PGCSKTHLPGFVQQAQELRSKGI
	Poecilia reticulata			PGCSKTHLPGFVQQAQELRSKGI
	Poecilia formosa			PGCSKTHLPGFVQQAQELRSKGI
	Stegastes partitus			PGCSKTHLPGFVQQAGDLKAKGI
	Oreochromis niloticus			PGCSKTHLPGFVQQAAELKNKGI
	Neolamprologus brichardi			PGCSKTHLPGFVEQAAELKNKGI
	Haplochromis burtoni	-		PGCSKTHLPGFVEQAAELKNKGI
	Maylandia zebra			'PGCSKTHLPGFVEQAAELKNKGI
	Pundamilia nyererei			'PGCSKTHLPGFVEQAAELKNKGI
	Sparus aurata			'PGCSKTHLPGFVEQASELKGKGI
	Miichthys miiuy			'PGCSKTHLPGFVEQAVELKSKGI
Prdx5:	Larimichthys crocea			PGCSKTHLPGFVEQAEALKSKGV ************************************
Prdx5:	Homo sapiens	AIPAVEVFEGEPGNKVNLAELFF	KGKKGVLFGVPGAFT	PGCSKTHLPGFVEQAEALKAKGV
Drdv5.	Trematomus bernacchii	OFVACTSVNDAFVMAAWGKEHG	A DCK T DMT A DDTCA E	TKAVDLLLDSDQIVQALGNKRSK
	Cynoglossus semilaevis			TKAVDLLISNDOLEOVLGNKRSK
	Takifugu rubripes			TKAVDLLLDSEELVQVLGNKRSK
	Fundulus heteroclitus			'AKAVDLLLDSDQIVQALGNHRSK
	Xiphophorus maculatus			'AKAVDLLLDSDTIVQVLGNKRSK
	Poecilia reticulata			'AKAVDLLLDSDTIVQVLGNKRSK
	Poecilia formosa			'AKAVDLLLDSDTIVQVLGNKRSK
	Stegastes partitus			TKAVDLLLDSEQIVQVLGNKRSK
	Oreochromis niloticus	-		TKAVDLLLDNDQIVQVLGNKRSK
	Neolamprologus brichardi			TKAVDLLLDIDQIVQVLGNKRSK
	Haplochromis burtoni			TKAVDLLLDSDQIVQVLGNKRSK
	Maylandia zebra			TKAVDLLLDSDQIVQVLGNKRSK
	Pundamilia nyererei			TKAVDLLLDSDQIVQVLGNKRSK
	Sparus aurata	~		TKAVDLLLDSDQIVQVLGNKRSK
	Miichthys miiuy	_		'AKAVDLLLDSDQIVQVLGNKRSK
	Larimichthys crocea			'AKAVDLLLDSDQIVQVLGNKRSK
IIUAJ.	Barrimrenenys erecea			**************************************
Prdx5:	Homo sapiens	QVVACLSVNDAFVTGEWGRAHKA	AEGKVRLLADPTGAF	GKETDLLLD-DSLVSIFGNRRLK
Prd×5·	Trematomus bernacchii	RYAMVVEDGVVKKINVEPDGTG	TCSLASNVI.SEL	
	Cvnoqlossus semilaevis	RYAMLVEDGVVKKINVEPDGTG		
	Takifugu rubripes	RYAMLVEDGVVKKINVEPDGTG	_~_	
	Fundulus heteroclitus	RYAMLVEDGVVKKINVEPDGTG		
	Xiphophorus maculatus	RYAMLVEDGVVKKINVEPDGTG		
	Poecilia reticulata	RYAMLVEDGVVKKINVEPDGTG		
	Poecilia formosa	RYAMLVEDGVVKKINVEPDGTG		
	Stegastes partitus	RYSMLVEDGVVKKLNVEPDGTG		
	Oreochromis niloticus	RYSMLVEDGVVKKLNVEPDGTG		
	Neolamprologus brichardi	RYSMLVEDGVVKKLNVEPDGTG		
	Haplochromis burtoni	RYSMLVEDGVVKKLNVEPDGTG		
	Maylandia zebra	RYSMLVEDGVVKKLNVEPDGTG		
	Pundamilia nyererei	RYSMLVEDGVVKKLNVEPDGTG		
	Sparus aurata	RYSMLVEDGVVKKINVEPDGTG		
	Miichthys miiuy	RYSMLVEDGVVKKVNVEPDGTG		
	Larimichthys crocea	RYSMLVEDGVVKKVNVEPDGTG		
	2	**:*:******		
Prdx5:	Homo sapiens	RFSMVVQDGIVKALNVEPDGTG		

Fig. 4. Multiple alignment of the amino acid sequences of 16 Prdx5s from Teleost species as well as from *Homo sapiens*. The amino acid residues highlighted in dark grey represent the peroxidase triad. The peroxidatic and the resolving cysteines are highlighted in light grey. Mitochondrial targeting signal is underlined. Peroxisomial targeting signal is double underlined. The symbols at the bottom of the Teleost sequences correspond to the definitions of the MUSCLE program: (*) fully conserved; (:) highly conserved; (.) conserved substitution.

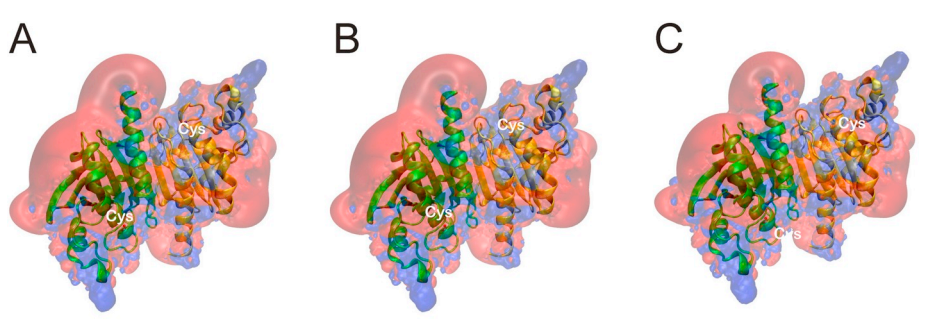


Fig. 5. Potential isosurfaces are shown at +3 kT/e in blue and -3 kT/e in red for Prdx3 of *T. bernacchii*, *N. coriiceps* and *S. partius* (panels A, B and C, respectively) and Prdx5 of *T. bernacchii* and *S. partius* (panels D and E, respectively). The positions of peroxidatic cysteines are reported. (For interpretation of the references to color in this figure legend, the reader is referred to the web version of this article.)

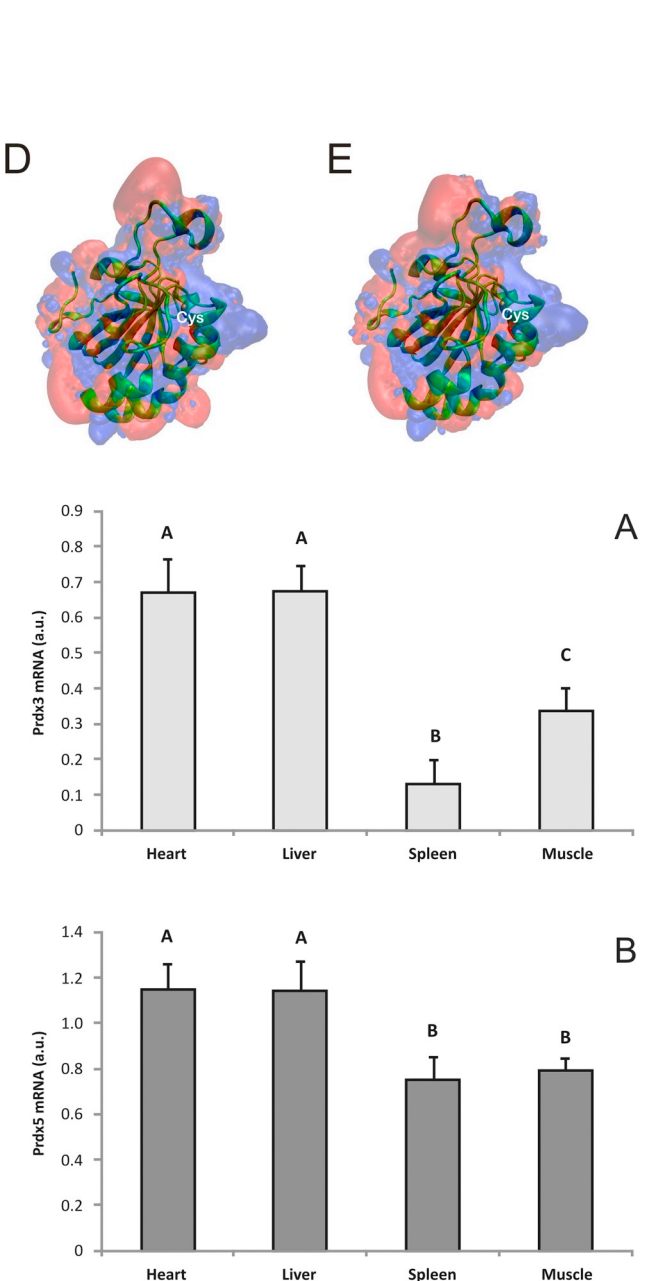


Fig. 6. mRNA levels in heart, liver, spleen and skeletal muscle of *Trematomus bernacchii* for prdx3 (A) and prdx5 (B). Letters: Student–Newman–Keuls t-test with respect to tissues (p < 0.05).

group during the entire experiment.

The mRNA level of both prdx3 and prdx5 remained constant during the entire experiment in heart tissues of control specimens (Fig. 8). On the contrary, the specimens exposed to short-term thermal stress showed, to some extent, temperature-dependent variations. In particular, the prdx3 mRNA levels increased at +2 °C (day 10, p < 0.05) and remain almost unchanged up to +3 °C (day 15; Fig. 8A). In both cases, the differences were statistically significant with respect to controls (p < 0.001). At +4 °C (day 20) the mRNA expression levels of prdx3 decreased, reaching values similar to controls. However, at +5 °C (day 25) its expression levels increased again (p < 0.05), nearly doubling with respect to controls (p < 0.001), showing a trend similar to those measured at +2°C (day 10). The prdx5 mRNA levels remained relatively constant during the first phases of the stress treatment, without showing any significant difference compared with controls. However, this transcript displayed a significant decrease at +4 °C (day 20, p < 0.05), reaching values 4-fold lower than controls (p < 0.001), only to return to its initial values, similar to controls at +5 °C (day 25; Fig. 8B).

4. Discussion

The present work reports the characterization of mitochondrial Prdxs in the Antarctic fish *T. bernacchii*. Phylogenetic analyses indicate that the evolution of these two newly identified isoforms has proceeded in parallel with the evolution of fish orders. The phylogenetic trees obtained from the coding sequences of Prdx3 and Prdx5 displayed similar topologies, at least for what concerns Cichliformes, Cyprinodontiformes and Perciformes. In fact, the sequences of these taxa were grouped in three well-supported clades. As expected, the Prdx sequences of *T. bernacchii* clustered in the Perciformes clade in both

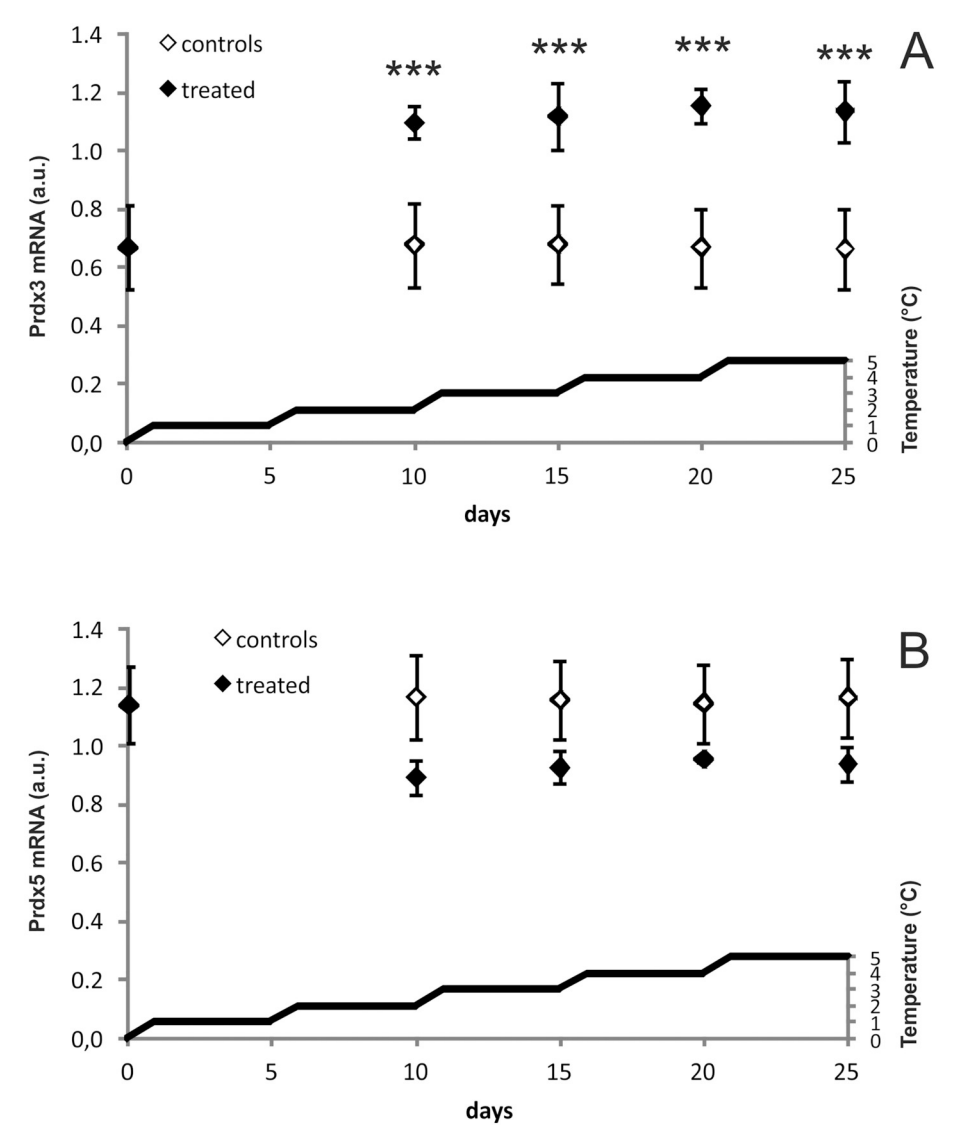


Fig. 7. Accumulation of prdx3 (A) and prdx5 (B) mRNAs in liver of T. bernacchii in response to environmental temperature increase. Asterisks: significant differences with respect to controls (***p < 0.001, **p < 0.005, *p < 0.05).

trees, mirroring the findings of a previous study based on the analysis of Prdx6s (Tolomeo et al., 2016). However, the relative position of the three aforementioned clades varied significantly in the two phylogenetic trees. In particular, the Cyprinodontiformes clade was identified as a sister group of Cichliformes in the Prdx3 phylogeny, whereas it was placed a sister group of Perciformes in the Prdx5 phylogeny. These branching patterns were different for Prdx6, where the sequences of Cichliformes and Perciformes constituted two sister groups. The discrepancies observed between Prdx3, Prdx5 and Prdx6 phylogenies (Tolomeo et al., 2016), can be most likely explained by independent evolutionary history of the three isoforms, characterized by their appearance at different times, through independent gene duplications, which may have occurred after the speciation events that led to the differentiation of extant teleost orders.

The analysis of Prdx amino acid sequences led to similar results, pointing out a significant impact of purifying selection on the evolution of both Prdx3s and Prdx5s, a hypothesis which is also supported by the results of MEC analyses. In fact, although some amino acid residues showed signatures of positive selection, they were all located within the N-terminal mitochondrial translocation signal, hence not covering a significant role in the catalytic activity of these enzymes. The action of purifying selection is important for the evolution of gene families, as it

guarantees the maintenance of function of the encoded proteins. However, positive selection is an important source of evolutionary innovation and it has been often advocated as a major force underlying the adaptation of species to new environments (Kosiol et al., 2008). A large number of protein families have experienced significant positive selection along their evolution, including those involved in immunity, reproduction and cell signaling (Bakiu et al., 2015a, 2015b). Although some studies have previously suggested that Prdxs may have evolved under positive selection (Bakiu and Santovito, 2015), our results indicate that this phenomenon is unlikely to have played a significant role in the evolution of these antioxidant enzymes, even though it may have acted episodically to sustain the functional diversification of variants, as in the case of Prdx6s (Tolomeo et al., 2016).

The multiple sequence alignment highlighted the presence of a number of amino acid substitutions unique to the mitochondrial *T. bernacchii* Prdx isoforms, which may be directly linked to cold adaptation, as previously reported for Prdx6A (Berthelot et al., 2018; Römisch and Matheson, 2003; Siddiqui and Cavicchioli, 2006). Among those referred to Prdx3, Ala⁷, Ser¹⁷, Lys¹⁰⁹, Leu¹²⁷ and Gln¹⁹² are substituted by Pro, His, Arg, Ile or Val and Lys, respectively (the first four substitutions are shared by the *N. coriiceps* Prdx3). Only the last two amino acids are in the proximity of functional residues of the

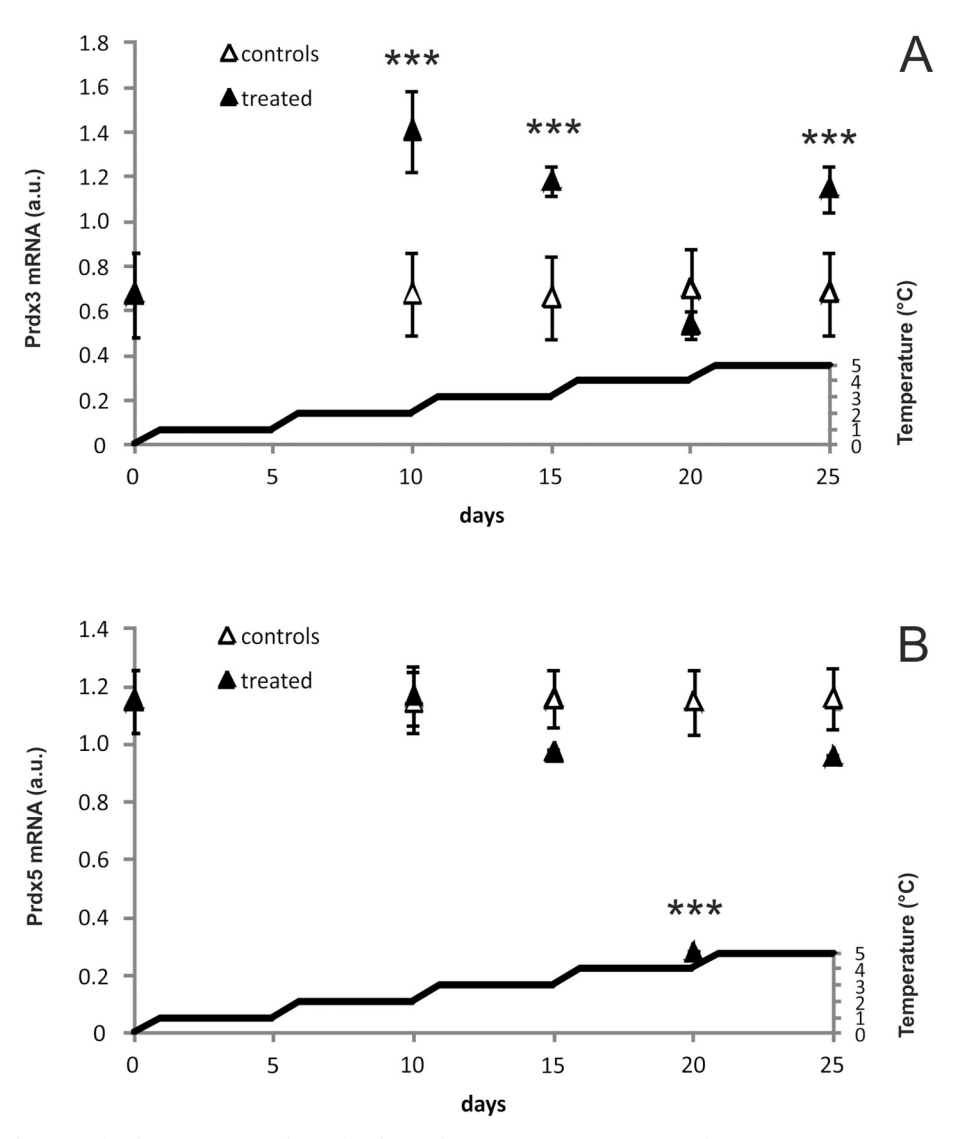


Fig. 8. Accumulation of prdx3 (A) and prdx5 (B) mRNAs in heart of T. bernacchii in response to environmental temperature increase. Asterisks: significant differences with respect to controls (***p < 0.001, **p < 0.005, *p < 0.05).

enzyme, i.e. the arginine of the catalytic triad and YF structural motif, which regulates the access of peroxide to peroxidatic cysteine. However, based on the chemical properties of the five substituted amino acids, none of these appear to confer more flexibility to the protein structure (Huang and Nau, 2003). Similar results were obtained in the analysis of Prdx5, where Met⁶⁵, Ile⁹³ and Val¹³¹ are substituted by Ile or Val, Val and Leu, respectively: only the last two residues potentially confer more flexibility to the enzyme, but they are located quite distantly from the regions of the protein responsible of for catalytic activity.

The new results provided by this study, together with those previously reported for Prdx6s, suggest that neither Prdx3, nor Prdx5 are "cold-adapted" enzymes. Homology modeling results seem to confirm this hypothesis, as the almost uniformly distributed negative charge of both isoforms closely matches those of "warm-adapted" Prdx6B (Tolomeo et al., 2016). Consistent with these observations, the predicted 3D structures of these mitochondrial Prdxs from *T. bernacchii* are almost identical to those of the tropical species *S. partitus*.

These features suggest a lower enzymatic activity of these two Prdx isoforms at low temperatures. Since the low temperatures of Antarctica promote the formation of ROS at higher rates, compared to temperate environments, the concentrations of hydrogen peroxide (the substrate of Prdxs) must be maintained at physiological levels in animals adapted

to this challenging environment. For this reason, cold adapted antioxidant enzymes that can vicariate the activity of Prdx3 and Prdx5 would be critical to the proper function of peroxisomes and mitochondria of this animal. In fact, these organelles must remain active in the cold even in relation to antioxidant defenses. Some studies have shown that glutathione peroxidase 1 (GPx-1) is present in mitochondria. This enzyme can modulate redox-dependent cellular responses by regulating mitochondrial function (Handy et al., 2009). Furthermore, the CAT enzyme has been reported to be exclusively located in the peroxisome matrix of fish hepatocytes (Orbea et al., 1999), indicating that these organelles may play a key role in lipid metabolism of fish liver

A recent publication demonstrated that the GPx-1 of *T. bernacchii*, shows features that may be related to low temperature adaptation. These include the presence of specific amino acid replacements that increase the number of polar residues, such as Arg, Glu, Ser, and Thr, and a high expression in liver and heart (Sattin et al., 2015). Additionally, our lab recently characterized the gene sequence and expression of CAT from Antarctic fish and found this enzyme is highly expressed in liver and heart and that many amino acids (about 3%) are conserved in Antarctic species only (in review). These residues are believed to be specifically involved in the formation tetrameric structures, such as the N-terminal threading arm and the C-terminal helical

domain, that are essential for the catalytic activity of this enzyme. Altogether, these observations suggest that enzymes characterized by structural features compatible with high catalytic activity at low temperatures, such as CAT and GPx-1, may represent a viable physiological alternative to the non-cold adapted Prdx3 and Prdx5 isoforms in *T. hernacchii*.

In addition, the gene expression data we collected for the *T. bernacchii* Prdx3 and Prdx5 orthologues indicated that these isoforms are only partially affected by temperature increase. When acclimated to temperatures as low as 3 °C, we observed a significant increase in Prdx3 transcription in both liver and heart tissues, which may represent a physiological antioxidant response of mitochondria against the formation of peroxides in this organelle during the thermal stress. Conversely, Prdx5 mRNA levels remained nearly stable in response to the same experimental thermal stress challenges.

Our results are consistent with previous studies which have shown that T. bernacchii experiences increased levels of oxidative damage during short-term thermal stress, likely as a result of elevated metabolic rates (Enzor and Place, 2014; Enzor et al., 2013; Garofalo et al., 2019). In fact, we have collected evidence that support an increase of the transcript levels for cytoplasmic superoxide dismutase (Cu,ZnSOD) in this species (in review). An increased Cu,ZnSOD activity, which converts superoxide ions into the less reactive species, H_2O_2 , is expected to result in the production of elevated levels of substrate for enzymes such as Prdxs and GPxs, which further reduce H_2O_2 . In addition to Prdx3, we also have recently obtained data that demonstrate an increase of the mRNA levels of Prdx6 (prdx6b gene) (Tolomeo et al., 2016) and GPx-1 (in review) in T. bernacchii, suggesting that this species is able to actively defends itself against ROS production under thermal stress.

The failure to induce *prdx5* in response to heat stress is probably related to the intracellular location of the protein encoded by this gene, which is also expressed in peroxisomes, besides mitochondria. Therefore, our results are compatible with an increased ROS production in mitochondria rather than peroxisomes.

In conclusion, we present here the first molecular and functional characterization of Prdx3 and Prdx5 in Antarctic fish, providing further contribution to the study of the antioxidant system in the ecological context of the Southern ocean (Santovito et al., 2006, 2000, 2012a, 2012b; Sattin et al., 2015; Tolomeo et al., 2016). Structural data seem to indicate that these enzymes are not "cold-adapted", a hypothesis further reinforced by the lack of inhibition of Prdx3 and Prdx5 to temperature changes. On the other hand, the rapid and specific response of Prdx3 to temperature increase reveals its potential usefulness as a biomarker of stress in environmental field studies related to global warming. Moreover, the activation of the Prdx3 expression in response to thermal stress may be a condition that limits the stenothermy of *T. bernacchii*, making this species less vulnerable to moderate environmental temperature changes and other environmental perturbations associated with global climate change.

Supplementary data to this article can be found online at https://doi.org/10.1016/j.cbpc.2019.108580.

Declaration of Competing Interest

The authors declare that they have no known competing financial interests or personal relationships that could have appeared to influence the work reported in this paper.

Acknowledgements

This research was supported by the Italian National Program for Antarctic Research (PNRA).

References

Acworth, I.N., McCabe, D.R., Maher, T., 1997. The analysis of free radicals, their reaction

- products and antioxidants. In: Baskin, S.I., Salem, H. (Eds.), Oxidants, Antioxidants and Free Radicals. Taylor and Francis, Washington, DC, pp. 23–77.
- Al-Asadi, S., Malik, A., Bakiu, R., Santovito, G., Menz, I., Schuller, K., 2019. Characterization of the peroxiredoxin 1 subfamily from *Tetrahymena thermophila*. Cell. Mol. Life Sci. https://doi.org/10.1007/s00018-019-03131-3.
- Baker, N.A., Sept, D., Joseph, S., Holst, M.J., McCammon, J.A., 2001. Electrostatics of nanosystems: application to microtubules and the ribosome. Proc. Natl. Acad. Sci. U. S. A. 98, 10037–10041.
- Bakiu, R., Santovito, G., 2015. New insights into the molecular evolution of metazoan peroxiredoxins. Acta Zool. Bulg. 67 (3), 305–317.
- Bakiu, R., Korro, K., Santovito, G., 2015a. Positive selection effects on the biochemical properties of mammal pyroglutamylated RFamide peptide receptor (QRFPR). It. J. Zool. 82, 309–326.
- Bakiu, R., Tolomeo, A.M., Santovito, G., 2015b. Positive selection effects on the biochemical properties of fish pyroglutamylated RFamide peptide receptor (QRFPR). It. J. Zool. 82, 460–472.
- Berthelot, C., Clarke, J., Desvignes, T., Detrich III, H.W., Flicek, P., Peck, L.S., Peters, M., Postlethwait, J.H., Clark, M.S., 2018. Adaptation of proteins to the cold in Antarctic fish: a role for methionine? Genome Biol. Evol. 11, 220–231.
- Biasini, M., Bienert, S., Waterhouse, A., Arnold, K., Studer, G., Schmidt, T., Kiefer, F., Gallo Cassarino, T., Bertoni, M., Bordoli, L., Schwede, T., 2014. SWISS-MODEL: modelling protein tertiary and quaternary structure using evolutionary information. Nucleic Acids Res. 42, W252–W258.
- Boldrin, F., Santovito, G., Formigari, A., Bisharyan, Y., Cassidy-Hanley, D., Clark, T.G., Piccinni, E., 2008. MTT2, a copper-inducible metallothionein gene from *Tetrahymena thermophila*. Comp. Biochem. Physiol. C 147, 232–240.
- Chae, H.Z., Kim, H.J., Kang, S.W., Rhee, S.G., 1999. Characterization of three isoforms of mammalian peroxiredoxin that reduce peroxides in the presence of thioredoxin. Diabetes Res. Clin. Pract. 45, 101–112.
- Clark, M.S., Peck, L.S., 2009. HSP70 heat shock proteins and environmental stress in Antarctic marine organisms: a mini-review. Mar. Genomics 2. 11–18.
- Darriba, D., Taboada, G.L., Doallo, R., Posada, D., 2011. ProtTest 3: fast selection of best-fit models of protein evolution. Bioinformatics 27, 1164–1165.
- Darriba, D., Taboada, G.L., Doallo, R., Posada, D., 2012. jModelTest 2: more models, new heuristics and parallel computing. Nat. Methods 9 (8), 772.
- heuristics and parallel computing. Nat. Methods 9 (8), 772.
 Dolinsky, T.J., Czodrowski, P., Li, H., Nielsen, J.E., Jensen, J.H., Klebe, G., Baker, N.A., 2007. PDB2PQR: expanding and upgrading automated preparation of biomolecular structures for molecular simulations. Nucleic Acids Res. 35, W522–W525.
- Doron-Faigenboim, A., Pupko, T., 2007. A combined empirical and mechanistic codon model. Mol. Biol. Evol. 24, 388–397.
- Edgar, R.C., 2004. MUSCLE: multiple sequence alignment with high accuracy and high throughput. Nucleic Acids Res. 32, 1792–1797.
- Enzor, L.A., Place, S.P., 2014. Is warmer better? Decreased oxidative damage in notothenioid fish after long-term acclimation to multiple stressors. J. Exp. Biol. 217, 3301–3310.
- Enzor, L.A., Zippay, M.L., Place, S.P., 2013. High latitude fish in a high CO₂ world: synergistic effects of elevated temperature and carbon dioxide on the metabolic rates of Antarctic notothenioids. Comp. Biochem. Physiol. A 164, 154–161.
- Ferro, D., Franchi, N., Mangano, V., Bakiu, R., Cammarata, M., Parrinello, N., Santovito, G., Ballarin, L., 2013. Characterization and metal-induced gene transcription of two new copper zinc superoxide dismutases in the solitary ascidian *Ciona intestinalis*. Aquat. Toxicol. 140-141, 369-379.
- Ferro, D., Bakiu, R., De Pitta, C., Boldrin, F., Cattalini, F., Pucciarelli, S., Miceli, C., Santovito, G., 2015. Cu,Zn superoxide dismutases from *Tetrahymena thermophila*: molecular evolution and gene expression of the first line of antioxidant defenses. Protist 166, 131–145.
- Ferro, K., Ferro, D., Corra, F., Bakiu, R., Santovito, G., Kurtz, J., 2017. Cu,Zn superoxide dismutase genes in *Tribolium castaneum*: evolution, molecular characterisation, and gene expression during immune priming. Front. Immunol. 8, 1811.
- Ferro, D., Franchi, N., Bakiu, R., Ballarin, L., Santovito, G., 2018. Molecular characterization and metal induced gene expression of the novel glutathione peroxidase 7 from the chordate invertebrate *Ciona robusta*. Comp. Biochem. Physiol. C 205, 1–7.
- Formigari, A., Boldrin, F., Santovito, G., Cassidy-Hanley, D., Clark, T.G., Piccinni, E., 2010. Functional characterization of the 5'-upstream region of MTT5 metallothionein gene from *Tetrahymena thermophila*. Protist 161, 71–77.
- Franchi, N., Ferro, D., Ballarin, L., Santovito, G., 2012. Transcription of genes involved in glutathione biosynthesis in the solitary tunicate *Ciona intestinalis* exposed to metals. Aquat. Toxicol. 114–115, 14–22. https://doi.org/10.1016/j.aquatox.2012.02.007.
- Garofalo, F., Santovito, G., Amelio, D., 2019. Morpho-functional effects of heat stress on the gills of Antarctic *T. bernacchii* and *C. hamatus*. Mar. Pollut. Bull. 141, 194–204.
- Gerdol, M., Buonocore, F., Scapigliati, G., Pallavicini, A., 2015. Analysis and characterization of the head kidney transcriptome from the Antarctic fish *Trematomus bernacchii* (Teleostea, Notothenioidea): a source for immune relevant genes. Mar. Genomics 20, 13–15.
- Guindon, S., Dufayard, J.F., Lefort, V., Anisimova, M., Hordijk, W., Gascuel, O., 2010. New algorithms and methods to estimate maximum-likelihood phylogenies: assessing the performance of PhyML 3.0. Syst. Biol. 59, 307–321.
- Hall, A., Karplus, P.A., Poole, L.B., 2009. Typical 2-Cys peroxiredoxins—structures, mechanisms and functions. FEBS J. 276, 2469–2477.
- Handy, D.E., Lubos, E., Yang, Y., Galbraith, J.D., Kelly, N., Zhang, Y.Y., Leopold, J.A., Loscalzo, J., 2009. Glutathione peroxidase-1 regulates mitochondrial function to modulate redox-dependent cellular responses. J. Biol. Chem. 284, 11913–11921.
- Hardy, A.C., Gunther, E.R., 1935. The Plankton of the South Georgia Whaling Grounds and Adjacent Waters 1926–1927. Cambridge University Press, Cambridge.
- Huang, F., Nau, W.M., 2003. A conformational flexibility scale for amino acids in peptides. Angew. Chem. Int. Ed. Eng. 42, 2269–2272.

- Huth, T.J., Place, S.P., 2013. De novo assembly and characterization of tissue specific transcriptomes in the emerald notothen, *Trematomus bernacchii*. BMC Genomics 14, 805.
- Irato, P., Piccinni, E., Cassini, A., Santovito, G., 2007. Antioxidant responses to variations in dissolved oxygen of *Scapharca inaequivalvis* and *Tapes philippinarum*, two bivalve species from the lagoon of Venice. Mar. Pollut. Bull. 54, 1020–1030.
- Johnston, I.I., Calvo, J., Guderley, Y.H., 1998. Latitudinal variation in the abundance and oxidative capacities of muscle mitochondria in perciform fishes. J. Exp. Biol. 201 (1), 1–12.
- Knoops, B., Goemaere, J., Van der Eecken, V., Declercq, J.P., 2011. Peroxiredoxin 5: structure, mechanism, and function of the mammalian atypical 2-Cys peroxiredoxin. Antioxid. Redox Signal. 15 (3), 817–829.
- Konig, J., Galliardt, H., Jutte, P., Schaper, S., Dittmann, L., Dietz, K.J., 2013. The conformational bases for the two functionalities of 2-cysteine peroxiredoxins as peroxidase and chaperone. J. Exp. Bot. 64, 3483–3497.
- Kosiol, C., Vinar, T., da Fonseca, R.R., Hubisz, M.J., Bustamante, C.D., Nielsen, R., Siepel, A., 2008. Patterns of positive selection in six mammalian genomes. PLoS Genet. 4, e1000144
- Kropotov, A., Sedova, V., Ivanov, V., Sazeeva, N., Tomilin, A., Krutilina, R., Oei, S.L., Griesenbeck, J., Buchlow, G., Tomilin, N., 1999. A novel human DNA-binding protein with sequence similarity to a subfamily of redox proteins which is able to repress RNA-polymerase-III-driven transcription of the Alu-family retroposons in vitro. Eur. J. Biochem. 260, 336–346.
- Legg, S., Briegleb, B., Chang, Y., Chassignet, E.P., Danabasoglu, G., Ezer, T., Gordon, A.L., Griffies, S., Hallberg, R., Jackson, L., Large, W., Özgökmen, T.M., Peters, H., Price, J., Riemenschneider, U., Wu, W., Xu, X., Yang, J., 2009. Improving oceanic overflow representation in climate models: the gravity current entrainment climate process team. Bull. Am. Meteorol. Soc. 90, 657–670.
- Lindorff-Larsen, K., Piana, S., Palmo, K., Maragakis, P., Klepeis, J.L., Dror, R.O., Shaw, D.E., 2010. Improved side-chain torsion potentials for the Amber ff99SB protein force field. Proteins 78, 1950–1958.
- Liu, N.N., Liu, Z.S., Lu, S.Y., Hu, P., Li, Y.S., Feng, X.L., Zhang, S.Y., Wang, N., Meng, Q.F., Yang, Y.J., Tang, F., Xu, Y.M., Zhang, W.H., Guo, X., Chen, X.F., Zhou, Y., Ren, H.L., 2015. Full-length cDNA cloning, molecular characterization and differential expression analysis of peroxiredoxin 6 from *Ovis aries*. Vet. Immunol. Immunopathol. 164, 208–219
- Notredame, C., Higgins, D.G., Heringa, J., 2000. T-coffee: a novel method for fast and accurate multiple sequence alignment. J. Mol. Biol. 302, 205–217.
- Orbea, A., Beier, K., Völkl, A., Dariush Fahimi, H., Cajaraville, M.P., 1999. Ultrastructural, immunocytochemical and morphometric characterization of liver peroxisomes in gray mullet, *Mugil cephalus*. Cell Tissue Res. 297, 493–502.
- Pörtner, H.O., Langenbuch, M., Michaelidis, B., 2005. Synergistic effects of temperature extremes, hypoxia, and increases in CO₂ on marine animals: from Earth history to global change. J. Geophys. Res. 110, C09S1.
- Rahaman, H., Zhou, S., Dodia, C., Feinstein, S.I., Huang, S., Speicher, D., Fisher, A.B., 2012. Increased phospholipase A2 activity with phosphorylation of peroxiredoxin 6 requires a conformational change in the protein. Biochemistry 51, 5521–5530.
- Randall, L.M., Ferrer-Sueta, G., Denicola, A., 2013. Peroxiredoxins as preferential targets in $\rm H_2O_2$ -induced signaling. Methods Enzymol. 527, 41–63.
- Ren, L., Sun, Y., Wang, R., Xu, T., 2014. Gene structure, immune response and evolution: comparative analysis of three 2-Cys peroxiredoxin members of miiuy croaker,

- Miichthys miiuy. Fish Shellfish Immunol. 36, 409-416.
- Ricci, F., Lauro, F.M., Grzymski, J.J., Read, R., Bakiu, R., Santovito, G., Luporini, P., Vallesi, A., 2017. The anti-oxidant defense system of the marine polar ciliate *Euplotes nobilii*: characterization of the MsrB gene family. Biology 6, 4.
- Römisch, K., Matheson, T., 2003. Cell biology in the Antarctic: studying life in the freezer. Nat. Cell Biol. 5 (1), 3–6.
- Ronquist, F., Teslenko, M., van der Mark, P., Ayres, D.L., Darling, A., Hohna, S., Larget, B., Liu, L., Suchard, M.A., Huelsenbeck, J.P., 2012. MrBayes 3.2: efficient Bayesian phylogenetic inference and model choice across a large model space. Syst. Biol. 61, 539–542
- Santovito, G., Irato, P., Piccinni, E., Albergoni, V., 2000. Relationship between metallothionein and metal contents in red-blooded and withe-blooded Antarctic teleosts. Polar Biol. 23 (6), 383–391.
- Santovito, G., Salvato, B., Manzano, M., Beltramini, M., 2002. Copper adaptation and methylotrophic metabolism in *Candida boidinii*. Yeast 19, 631–640.
- Santovito, G., Piccinni, E., Cassini, A., Irato, P., Albergoni, V., 2005. Antioxidant responses of the Mediterranean mussel, Mytilus galloprovincialis, to environmental variability of dissolved oxygen. Comp. Biochem. Physiol. C 140, 321–329.
- Santovito, G., Cassini, A., Piccinni, E., 2006. Cu,Zn superoxide dismutase from Trematomus bernacchii: functional conservation and erratic molecular evolution in Antarctic teleosts. Comp. Biochem. Physiol. C 143, 444–454.
- Santovito, G., Marino, S.M., Sattin, G., Cappellini, R., Bubacco, L., Beltramini, M., 2012a. Cloning and characterization of cytoplasmic carbonic anhydrase from gills of four Antarctic fish: insights into the evolution of fish carbonic anhydrase and cold adaptation. Polar Biol. 35, 1587–1600.
- Santovito, G., Piccinni, E., Boldrin, F., Irato, P., 2012b. Comparative study on metal homeostasis and detoxification in two Antarctic teleosts. Comp. Biochem. Physiol. C 155, 580-586.
- Santovito, G., Boldrin, F., Irato, P., 2015. Metal and metallothionein distribution in different tissues of the Mediterranean clam *Venerupis philippinarum* during copper treatment and detoxification. Comp. Biochem. Physiol. C 174–175, 46–53. https://doi.org/10.1016/j.cbpc.2015.06.008.
- Sattin, G., Bakiu, R., Tolomeo, A.M., Carraro, A., Coppola, D., Ferro, D., Patarnello, T., Santovito, G., 2015. Characterization and expression of a new cytoplasmic glutathione peroxidase 1 gene in the Antarctic fish *Trematomus bernacchii*. Hydrobiologia 761, 363–372.
- Seo, M.S., Kang, S.W., Kim, K., Baines, I.C., Lee, T.H., Rhee, S.G., 2000. Identification of a new type of mammalian peroxiredoxin that forms an intramolecular disulfide as a reaction intermediate. J. Biol. Chem. 275, 20346–20354.
- Shaw, G., Kamen, R., 1986. A conserved AU sequence from the 3' untranslated region of GM-CSF mRNA mediates selective mRNA degradation. Cell 46 (5), 659–667.
- Siddiqui, K.S., Cavicchioli, R., 2006. Cold-adapted enzymes. Annu. Rev. Biochem. 75, 403–433
- Tolomeo, A.M., Carraro, A., Bakiu, R., Toppo, S., Place, S.P., Ferro, D., Santovito, G., 2016. Peroxiredoxin 6 from the Antarctic emerald rockcod: molecular characterization of its response to warming. J. Comp. Physiol. B. 186, 59–71.
- Wood, Z.A., Poole, L.B., Karplus, P.A., 2003a. Peroxiredoxin evolution and the regulation of hydrogen peroxide signaling. Science 300, 650–653.
- Wood, Z.A., Schröder, E., Harris, J.R., Poole, L.B., 2003b. Structure, mechanism and regulation of peroxiredoxins. Trends Biochem. Sci. 28, 32–40.